

PREPARATION AND THERMAL DECOMPOSITION OF SYNTHETIC BAYERITE

N. Koga, T. Fukagawa and H. Tanaka

Chemistry Laboratory, Faculty of Education, Hiroshima University, 1-1-1 Kagamiyama, Higashi-Hiroshima 739-8524, Japan

Abstract

The formation process of bayerite, from an aqueous solution of sodium aluminate through enforced decomposition of aluminate ions by introducing CO₂ gas and aging with mechanical stirring, was investigated by pH measurements of the mother solution during preparation reaction and characterization of precipitates obtained at various stages of preparation. An amorphous precipitate, produced initially by the reaction of introduced CO₂, transformed to bayerite via pseudoboehmite during aging. It was found that the crystalline particle size and morphology of the crystallized bayerite change depending systematically on the preparation conditions. The reaction pathway of the thermal decomposition of the synthesized bayerite was investigated by using thermoanalytical techniques.

Keywords: formation process of bayerite, synthetic bayerite, thermal decomposition

Introduction

Aluminum hydroxides and oxyhydroxides are important as precursors of aluminum oxides for various industrial purposes. Preparation methods and thermal decomposition processes of crystalline aluminum hydroxides and oxyhydroxides have been studied by many workers [1]. The thermal decomposition processes are different in their polymorphic crystals and in many cases very complicated, producing α -Al₂O₃ via various transitional aluminum oxides [2].

Diverse aluminum oxide and hydroxide phases have been produced from sodium aluminate solutions [1, 3, 4]. Although the influence of the preparation conditions on the resulting phase has widely been examined, details of the formation process of a particular phase have not been established yet. Further knowledge on the formation process is useful to control the process and properties of the resulting phase. In the present study, the formation process of bayerite, from an aqueous solution of sodium aluminate through enforced decomposition of aluminate ions by introducing CO₂ gas, was investigated through pH measurements of the mother solution during preparation reaction and characterization of precipitates obtained at various stages of the reaction. Influence of preparation conditions on the formation process and resulting bayerite was investigated. The thermal decomposition processes of the samples with different particle sizes were studied by thermoanalytical techniques.

Experimental

Sample preparation

Carbon dioxide was introduced, at a rate of 100 mL min^{-1} , into 500 mL of sodium aluminate solutions (0.3–1.2 M) at 300 K until the pH value of the solution is down to various predetermined values. With mechanical stirring, precipitates produced during the carbonation process were aged in the mother solution at 300 K. During the preparation reaction, pH of the mother solution was monitored using Horiba PH-22. Several characteristic behaviors in the pH variation of the mother solution were observed during the preparation reaction. The precipitates obtained at various characteristic stages of preparation reaction were filtered and washed with water, and drying in vacuum desiccators.

Characterization

Powder X-ray diffraction (XRD) patterns of the precipitates were recorded with a Geigerflex RAD-B (Rigaku) using Ni-filtered $\text{CuK}\alpha$ radiation (30 kV, 15 mA). Fourier transform infrared spectroscopy (FT-IR) was measured by diffuse reflectance using a FTIR-8100M (Shimadzu) for samples mixed with KBr (3 mass% sample with 97 mass% KBr). The samples lightly coated by Au evaporation were observed by scanning electron microscopy (SEM) using a JSM-T20 (Jeol). Specific surface areas of the sample were evaluated by a BET single point method with FlowSorb II 2300 (Micromeritics) using He-N_2 standard gas. TG-DTA measurements were performed using a TGD-7600 (ULVAC) at a heating rate of 10 K min^{-1} under flowing N_2 (80 mL min^{-1}). Constant rate thermal analysis (CRTA) was carried out using remodeled Shimadzu TGA-50 under flowing N_2 (80 mL min^{-1}). The thermal decomposition of crystalline bayerite was followed by high-temperature XRD of a RINT2200 equipped with a heating chamber (Rigaku) using monochromed $\text{CuK}\alpha$ radiation (40 kV, 20 mA).

Results and discussion

Figure 1 shows the pH variation of the mother solution, 0.3 M sodium aluminate solution, during the carbonation procedure and subsequent aging with mechanical stirring. By introducing CO_2 gas, pH of the mother solution decreased rapidly by the neutralization of the free base present in the system. An inflection point on the pH curve, observed at $\text{pH}=11.3$, seems to correspond to the end of neutralization reaction. The mother solution changed to a white colloidal solution at around the inflection point. Further introduction of CO_2 caused visible precipitate with gradual decrease in pH. Even when CO_2 introduction was stopped before the inflection point, pH of the solution decreased continuously to the inflection point and indicated a nearly constant pH value at around the pH value of the inflection point for a while during aging. For the solution with further introduction of CO_2 beyond the inflection point, pH decreased

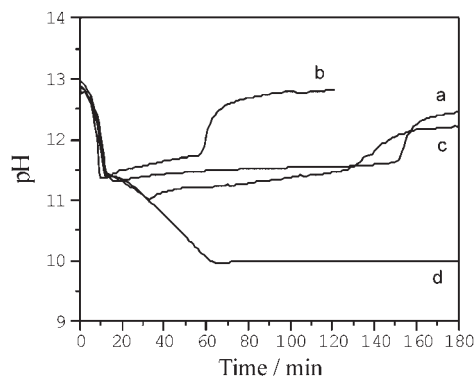


Fig. 1 Time-dependent change in pH of sodium aluminate solution (0.3 M) during aging after introducing CO₂ until various pH, a – 12.0, b – 11.5, c – 11.0 and d – 10.0 are reached

gradually until CO₂ introduction was stopped and the pH value was maintained during aging. After a period of stable pH, rapid increase in pH of the solution was observed for all the measurements.

Figure 2 compares XRD patterns for the precipitate obtained at the inflection point, during aging with mechanical stirring at a constant pH and after the rapid increase in pH. No distinguished diffraction peak was observed for the colloidal precipitates obtained at the inflection point of pH. The gelatinous precipitate obtained during the mechanical stirring of the mother solution indicated broad diffraction peaks due to pseudoboehmite. After rapid increase in pH of the mother me-

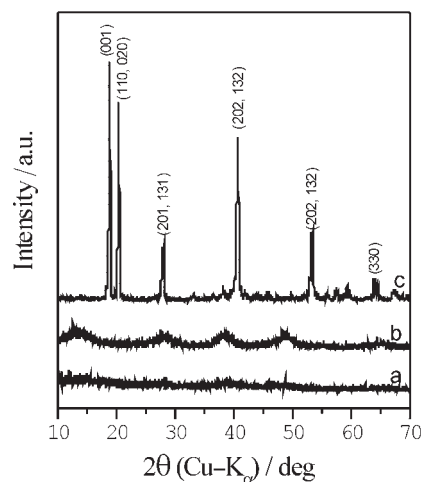


Fig. 2 Typical XRD patterns for the precipitates obtained at the characteristic stages in the preparation process, a – at the inflection point of pH, b – during aging and c – after rapid increase in pH

chanical stirring was observed, the precipitate turned out to show a well-distinguished XRD pattern of crystalline aluminum hydroxide, i.e., bayerite.

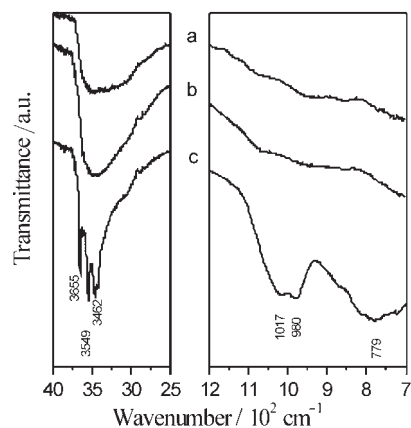


Fig. 3 Typical FTIR spectra for the precipitates obtained at the characteristic stages in the preparation process, a – at the inflection point of pH, b – during aging and c – after rapid increase in pH

Figure 3 shows FT-IR spectra for the corresponding precipitates. A single broad band due to O–H stretching vibration around $3000\text{--}3700\text{ cm}^{-1}$ observed for the gelatinous precipitate splits into several distinguished peaks after rapid increase in pH of the mother solution during mechanical stirring. In addition, OH bending bands at 1017 and 980 cm^{-1} and a broad band centered at around $770\text{--}720\text{ cm}^{-1}$, due to Al–OH group, are clearly observed for the crystallized precipitate. The IR spectrum of the crystallized precipitate is in good agreement with absorption due to bayerite.

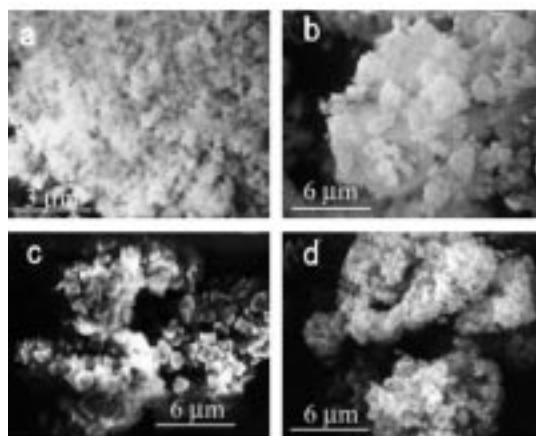


Fig. 4 Typical SEM images for the precipitates obtained at characteristic stages in the preparation process, a – amorphous precipitate, b – pseudoboehmite, c – bayerite from 0.3 M mother solution, and d – bayerite from 1.2 M mother solution

SEM images of the precipitates are shown in Fig. 4a–c. The X-ray amorphous precipitate obtained at the inflection point of pH shows aggregates of very fine particles. It is clear by comparing Fig. 4a and b that the particle size of the gelatinous precipitate increases during mechanical stirring. After crystallization, the precipitate exhibits aggregates of well-shaped crystals. Such observations indicate that the amorphous precipitates produced at the end of neutralization reaction transforms to pseudoboehmite by increasing the particle size during the mechanical stirring of the mother solution. The suspension of pseudoboehmite suddenly crystallizes to bayerite after a certain aging time. The present formation behavior is in qualitative agreement with the reported formation behavior that bayerite phase formation can be explained by the aging of amorphous or pseudoboehmite phases contained in the gelatinous precipitate [5].

Influences of concentration of the mother solution on the formation process and resulting bayerite were examined. As listed in Table 1, the carbonation procedure was performed, using mother solutions with different concentrations, until pH values of the mother solution decrease to a predetermined value that is slightly higher than that at the inflection point of pH. Even after the carbonation procedure stopped, pH of the mother solution decreased to the value at the inflection point of the respective solution with different concentrations. Experimental duration time from the inflection point of pH to the onset point of pH variation due to crystallization was also listed in Table 1 as ‘Induction period for crystallization’. The induction period decreases with increasing the concentration of the mother solution. Irrespectively of the concentration of the mother solution, the crystallized phase was identified by XRD and FTIR as bayerite. Specific surface areas of as-prepared bayerite increased with increasing the concentration of the mother solution. Figure 4(c) and (d) compares SEM image of as-prepared bayerite from mother solutions with different concentrations. The precipitates were recognized as aggregates of crystalline particles and the particle size increased with the decreasing concentration of the mother solution.

Table 1 Influences of concentration of the mother solution, *c*, on the formation process and resulting bayerite

<i>c</i> / M	pH		<i>t</i> _{indux} ^c /min	<i>S</i> _{BET} ^d /m ² g ⁻¹
	CO ₂ ^a	Inflex. ^b		
0.3	12.0	11.3	131	1.2
0.6	12.3	11.8	20	6.9
0.9	12.3	12.0	7	12.6
1.2	12.5	12.3	6	15.5

^apH value when CO₂ introduction was stopped

^bpH value at the inflection point

^cInduction period for crystallization of bayerite

^dSpecific surface area of resulting bayerite

Figure 5 shows typical TG-DTA curves for the thermal decomposition of synthetic bayerite prepared from the mother solution of 0.3 and 1.2 M. Irrespectively of

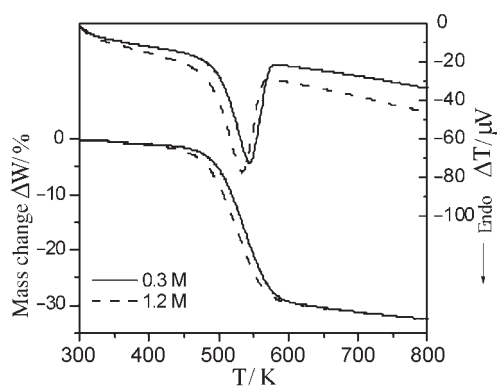


Fig. 5 Typical TG-DTA curves for the thermal decomposition of bayerite (20.0 mg) at a heating rate of 5.0 K min^{-1} under flowing N_2 at 80 mL min^{-1} . Solid and broken lines are for the samples obtained from the mother solutions of 0.3 and 1.2 M, respectively

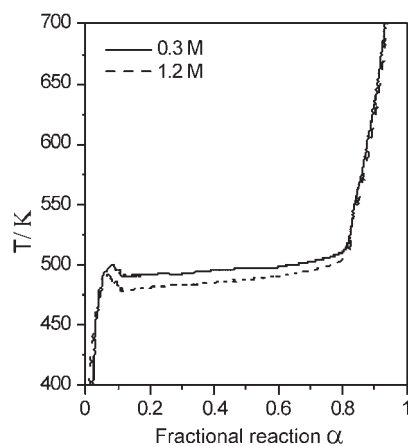


Fig. 6 Typical temperature profiles of CRTA curves for the thermal decomposition of bayerite (15.0 mg) at a controlled rate of $1.5 \cdot 10^{-2} \text{ mg min}^{-1}$ under flowing N_2 at 80 mL min^{-1} . Solid and broken lines are for the samples obtained from the mother solutions of 0.3 and 1.2 M, respectively

the samples, the total mass loss determined by heating from room temperature to 1100 K was in good agreement with the theoretical value for the thermal decomposition of aluminum hydroxide to aluminum oxide, 34.6%. As is clearly seen by comparing temperatures at DTA endothermic peaks, the reaction temperatures shifted to the higher temperature region for the sample prepared from the mother solution of lower concentration. The behavior is expected from the larger particle size of the sample prepared from mother solution of lower concentration. Irrespectively of the samples, the mass loss trace indicated an inflection point at the fractional reaction of about 80%, followed by gradual mass loss completed at around 1100 K. The samples

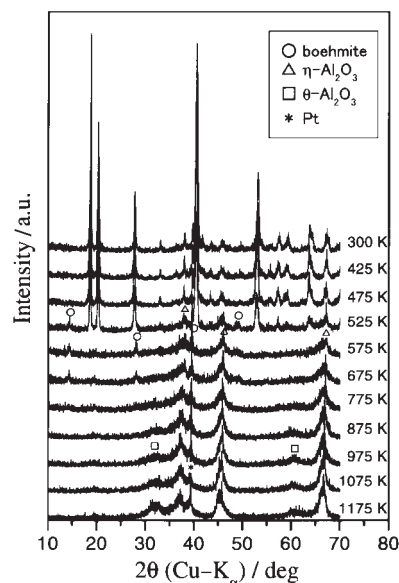


Fig. 7 Change in XRD patterns during the thermal decomposition of bayerite obtained from 0.3 M solution

were also subjected to CRTA measurement. Figure 6 shows typical temperature profiles for the thermal decomposition of the samples at a controlled rate of $2.0 \cdot 10^{-2} \text{ mg min}^{-1}$. At the fractional reaction of about 80%, an apparent temperature jump is observed for both the samples, indicating a possible change of the reaction step and/or kinetics.

Change in XRD patterns of the sample, during linear heating at 5 K min^{-1} under flowing N_2 at a rate of 100 mL min^{-1} , was shown in Fig. 7. As an intermediate compound of the thermal decomposition, the boehmite phase is identified around 525–675 K. During the gradual mass loss stage after the inflection point of mass loss trace, the boehmite phase decomposes to $\eta\text{-Al}_2\text{O}_3$. Before completing the mass loss due to the thermal decomposition of boehmite, the decomposition product $\eta\text{-Al}_2\text{O}_3$ transforms partially to $\theta\text{-Al}_2\text{O}_3$. On further heating, these transitional aluminas crystallized to form $\alpha\text{-Al}_2\text{O}_3$ above 1450 K. The similar reaction pathway of the thermal decomposition of synthetic bayerite has already been reported by other workers [2, 6, 7]. Recently, it has been found in our experimental work that the reaction pathway and kinetics of the thermal decomposition vary systematically depending on the reaction conditions applied. The details of the reaction behavior will be reported elsewhere.

Conclusions

- An initially produced amorphous precipitate by introduction of CO_2 into a sodium aluminate solution transforms to pseudoboehmite during aging of the suspension

with mechanical stirring. After a certain induction period, the precipitate crystallizes to form bayerite.

- The formation process and morphology of resulting bayerite are influenced by the concentration of sodium aluminate solution.
- Under flowing N_2 , bayerite decomposes thermally to $\eta-Al_2O_3$ via boehmite.

References

- 1 Hector Juarez M., J. Merced Martinez R., J. Manuel Ruvalcaba L., Oriana A. Vargas P. and Juan Serrato R., *Am. Ceram. Soc. Bull.*, 76 (1997) 55.
- 2 H. C. Stumpf, *Ind. Eng. Chem.*, 42 (1950) 1398.
- 3 V. H. Ginsberg, W. Huttig and H. Stiehl, *Z. anorg. allg. Chem.*, 309 (1961) 16.
- 4 M. Pyzalsky, M. Wojcik and R. Urbansky, *Light Met.*, (1992) 131.
- 5 A. van Straten, B. T. W. Holtkamp and P. L. de Bruyn, *J. Colloid Interface Sci.*, 98 (1984) 348.
- 6 T. Sato, *J. Appl. Chem.*, 12 (1962) 553.
- 7 T. Tsuchida and N. Ichikawa, *React. Solids*, 7 (1989) 207.